Received: 19 June 2019 | Accepted: 3 October 2019
DOI: 10.1002/hyp.13608

RESEARCH ARTICLE

WILEY

Influence of landscape and hydrological factors on stream–air temperature relationships at regional scale

Aurélien Beaufort[1,2] | Florentina Moatar[2] | Eric Sauquet[2] | Pierre Loicq[1] | David M. Hannah[3]

[1]EA 6293 GéHCO Géo-Hydrosystèmes Continentaux, Université François-Rabelais de Tours, Parc de Grandmont, Tours, 37200, France
[2]UR RiverLy, Irstea, centre de Lyon-Villeurbanne, 5 rue de la Doua CS 20244, Villeurbanne, 69625, France
[3]School of Geography, Earth and Environmental Sciences, University of Birmingham Edgbaston, Birmingham, B15 2TT, United Kingdom

Correspondence
Aurélien Beaufort, UR RiverLy, Irstea, centre de Lyon-Villeurbanne, 5 rue de la Doua CS 20244, Villeurbanne 69625, France.
Email: aurelien.beaufort@irstea.fr

Funding information
French Agency for Biodiversity

Abstract

Identifying the main controlling factors of the stream temperature (*Tw*) variability is important to target streams sensitive to climate and other drivers of change. The thermal sensitivity (*TS*), based on relationship between air temperature (*Ta*) and *Tw*, of a given stream can be used for quantifying the streams sensitivity to future climate change. This study aims to compare *TS* for a wide range of temperate streams located within a large French catchment (110,000 km^2) using 4 years of hourly data (2008–2012) and to cluster stations sharing similar thermal variabilities and thereby identify environmental key drivers that modify *TS* at the regional scale. Two successive classifications were carried out: (a) first based on *Ta*–*Tw* relationship metrics including *TS* and (b) second to establish a link between a selection of environmental variables and clusters of stations. Based on weekly *Ta*–*Tw* relationships, the first classification identified four thermal regimes with differing annual *Tw* in terms of magnitude and amplitudes in comparison with *Ta*. The second classification, based on classification and regression tree method, succeeded to link each thermal regime to different environmental controlling factors. Streams influenced by both groundwater inflows and shading are the most moderated with the lowest *TS* and an annual amplitude of *Tw* around half of the annual amplitude of *Ta*. Inversely, stations located on large streams with a high distance from source and not (or slightly) influenced by groundwater inflows nor shading showed the highest *TS*, and so, they are very climate sensitive. These findings have implications for guiding river basin managers and other stakeholders in implementing thermal moderation measures in the context of a warming climate and global change.

KEYWORDS
CART method, classification, regional scale, stream temperature, thermal sensitivity

1 | INTRODUCTION

Water temperature (*Tw*) is a fundamental water quality parameter that controls aquatic community structure and affects ecological processes in rivers and streams (Caissie, 2006; Comte, Buisson, Daufresne, & Grenouillet, 2013; Jonsson & Jonsson, 2009; Webb, Hannah, Moore, Brown, & Nobilis, 2008). The impacts of global change on hydrosystems are potentially numerous and result from changes in extreme precipitation frequency and increased air temperature (*Ta*), evaporation, and dry periods (e.g., Garner, Hannah, & Watts, 2017; Watts et al., 2015). The rise of *Ta* is expected resulting in warmer stream *Tw* (Garner, Hannah, Sadler, & Orr, 2014; Hannah & Garner, 2015; Mohseni & Stefan, 1999; van Vliet et al., 2013), which could be exacerbated by the reducing of summer stream flows especially in temperate climate (Isaak et al., 2010; van Vliet et al., 2013). In France, several studies have already highlighted an increase in *Tw* across various rivers (Bustillo, Moatar, Ducharne, Thiéry, & Poirel, 2014; Jackson, Fryer, Hannah, & Malcolm, 2017; Jackson, Fryer, Hannah, Millar, & Malcolm, 2018; Jackson, Hannah, Fryer, Millar, & Malcolm, 2017; Moatar & Gailhard, 2006). There is therefore a growing interest in understanding the spatio-temporal variability of river thermal regime given the likely effects of climate change (increase of both the *Ta* and the evapotranspiration, shift in river flow regimes and of groundwater inflows, etc.; Webb et al., 2008; Moatar et al., 2010). The goal is to develop opportunities for mitigation and adaptive management of river systems (Boisneau, Moatar, Bodin, & Boisneau, 2008; Hrachowitz, Soulsby, Imholt, Malcolm, & Tetzlaff, 2010; Jackson, Malcolm, & Hannah, 2015; Kurylyk, MacQuarrie, Linnansaari, Cunjak, & Curry, 2015).

The *Tw* variability, described by metrics of flow magnitude, frequency, duration, timing, and rate of change, on various timescales (Jones & Schmidt, 2018), is influenced by complex processes related to atmospheric, hydrogeological, geomorphic, and landscape characteristics and anthropogenic pressures, which could interact at multiple spatial scales (Caissie, 2006; Hannah & Garner, 2015). Numerous studies have highlighted the importance of riparian forest and groundwater inflows in moderating *Tw* variability (Dugdale, Malcolm, Kantola, & Hannah, 2018; Garner, Malcolm, Sadler, & Hannah, 2017; Kelleher et al., 2012; Lalot et al., 2015; Loicq, Moatar, Jullian, Dugdale, & Hannah, 2018). Identifying the main controlling factors of *Tw* variability remains an important task to target streams sensitive to climate change and to develop mitigation action to preserve aquatic ecosystems (Jackson et al., 2018).

Classification and regression tree (CART) of hydrological and landscape-dependent variables are informative and revealing methods to answer explore patterns without introducing an a priori structure of the link between explanatory variables and metrics describing *Tw* variability (Arismendi, Johnson, Dunham, & Haggerty, 2013; Casado, Hannah, Peiry, & Campo, 2013; Chu, Jones, & Allin, 2009).

Some studies, in various parts of the world, considered explicitly and empirically the role of a limited number of basin properties on *Tw* (e.g., Garner et al., 2014; Hrachowitz et al., 2010; Jackson et al., 2015; Faye L. Jackson, Fryer, et al., 2017; Faye L. Jackson et al., 2018; Jackson, Hannah, et al., 2017 in the UK; Isaak & Hubert, 2001; Isaak et al., 2010; Nelitz, MacIsaac, & Peterman, 2007, in North America). Analyses in most of these studies are carried out on a site-by-site basis, which limits the extent to which broad patterns can be inferred (Laizé, Bruna Meredith, Dunbar, & Hannah, 2017). Some regional-scale studies have used spatial thermal regime classification based on a large set of catchment properties (Chu et al., 2009; Laizé et al., 2017; Maheu, Poff, & St-Hilaire, 2016; Rivers-Moore, Dallas, & Morris, 2013; Tague, Farrell, Grant, Lewis, & Rey, 2007). These studies succeeded in identifying key drivers that influence the thermal regime of streams at the regional scale. Most of these studies use on metrics summarizing the warmest aspects of the *Tw* regime to examine the threats to cold-water species under climate change.

Several researchers analyse the relationship between *Tw* and *Ta*, with *Ta* taken as a surrogate of the main climatic drivers (Ducharne, 2008; Garner et al., 2014). *Ta* is a common variable, easily measured on the field, and it is strongly correlated to solar radiation (Bustillo et al., 2014). Kelleher et al. (2012) studied the thermal sensitivity (*TS*) of streams to represent the relative sensitivity of *Tw* of a given stream to environmental change. *TS* is defined as the slope of the regression line between *Ta* and *Tw*, which can be linear (or logistic) and can be fitted on data averaged at different timescales (Mohseni & Stefan, 1999; O'Driscoll & DeWalle, 2006; Stefan & Preud'homme, 1993). *TS* summarizes the cumulative buffering effects of local landscape characteristics on stream temperatures. Although *TS* may evolve into the future due to the changing drivers considered above, *TS* computed for a specific period of record gives insight of which streams have the greatest sensitivity to climate based on contemporary conditions, which can be used as a baseline for responsiveness (Kelleher et al., 2012). However, this integrated variable cannot distinguish the cause and effect of groundwater and riparian vegetation shading on *Tw* variability (Chang & Psaris, 2013; Chu et al., 2009; O'Driscoll & DeWalle, 2006). Understanding the importance of these driving factors is essential to develop appropriate strategies to mitigate and adapt to stream heating under anticipated climate warming.

The aim of our study is (a) to provide a comparison of thermal sensitivity (*TS*) across a wide range of French temperate streams, based on 4 years of hourly data (2008–2012), and (b) to identify groups of streams with similar sensitivity and so infer the environmental key factors that control *TS* at the regional scale. For that purpose, two successive classifications of 127 stations located in the Loire catchment (Beaufort et al., 2016) were carried out: (a) first based on *Ta*–*Tw* relationship metrics including *TS* and (b) second to establish a link between a selection of environmental variables and thermal regimes of stations. Finally, the relative importance of environmental variables on the *TS* of streams is investigated, and the implication for river management and river restoration is discussed.

2 | MATERIAL AND METHODS

2.1 | Sites and temperature data

2.1.1 | Basin description

The Loire basin (Figure 1) comprises a hydrographical network of 88,000 km and drains a catchment area of 117,000 km^2. It is characterized by varying climates between the upstream and the downstream (annual rainfall between 550 and 2,100 mm/year and annual air temperature between 6°C and 12.5°C), landform (10% of the basin area >800 m; mean altitude = 300 m), and lithology (metamorphic, magmatic, and sedimentary rocks). The percentage of riparian vegetation, defined on a buffer zone of 10 m on both sides of the streams, is globally greater in the southern basin where the altitude is the highest (mean ratio of the riparian vegetation = 75%; dark green; Figure 1c). Streams located in the central part of the basin, mainly composed of sedimentary rocks, benefit more from groundwater contributions (Figure 1d). The main aquifers are found in the sedimentary rocks in the centre of the basin. The Beauce formations (12,700 km^2) are composed of many semipermeable aquifers (Mohseni & Stefan, 1999) with numerous groundwater inflows located at the north of the Loire basin. Some streams are very directly connected to this aquifer, and their flow depends on the level of the Beauce water table (Baratelli, Flipo, & Moatar, 2016).

2.1.2 | Field monitoring

Tw was monitored, hourly, at 127 stations managed by the French Agency for Biodiversity (http://www.naiades.eaufrance.fr), between July 2008 and December 2012, distributed across the Loire basin (Figure 1b). The monitoring stations are mainly located on streams with a Strahler order between 3 and 5 (78% of stations). All monitoring stations are located on streams with low direct human influence on the flow regime, and all time series of *Tw* have been scrutinized to discard streams influenced by dam operations. The mean annual water temperatures of these stations range from 7.5°C to 15.7°C. The highest mean annual temperatures were observed on large rivers such as the Loire (Strahler Order 8) and its main tributaries, where mean annual *Tw* ranged between 14°C and 15.7°C between 2008 and 2012 (Figure 1a; Beaufort et al., 2016). Colder temperatures (<9°C) were observed in the upstream reaches of the Loire River where the altitude is above 1,000 m. The annual *Tw* at stations located on small streams (51 stations <30 km from upstream sources) did not exceed 13°C (Figure 1b). Moreover, gaps in *Tw* time series between 2008 and 2012 exist, and the proportion of missing values is about 35% on average for the 127 stations (80 stations with more than 20% of missing

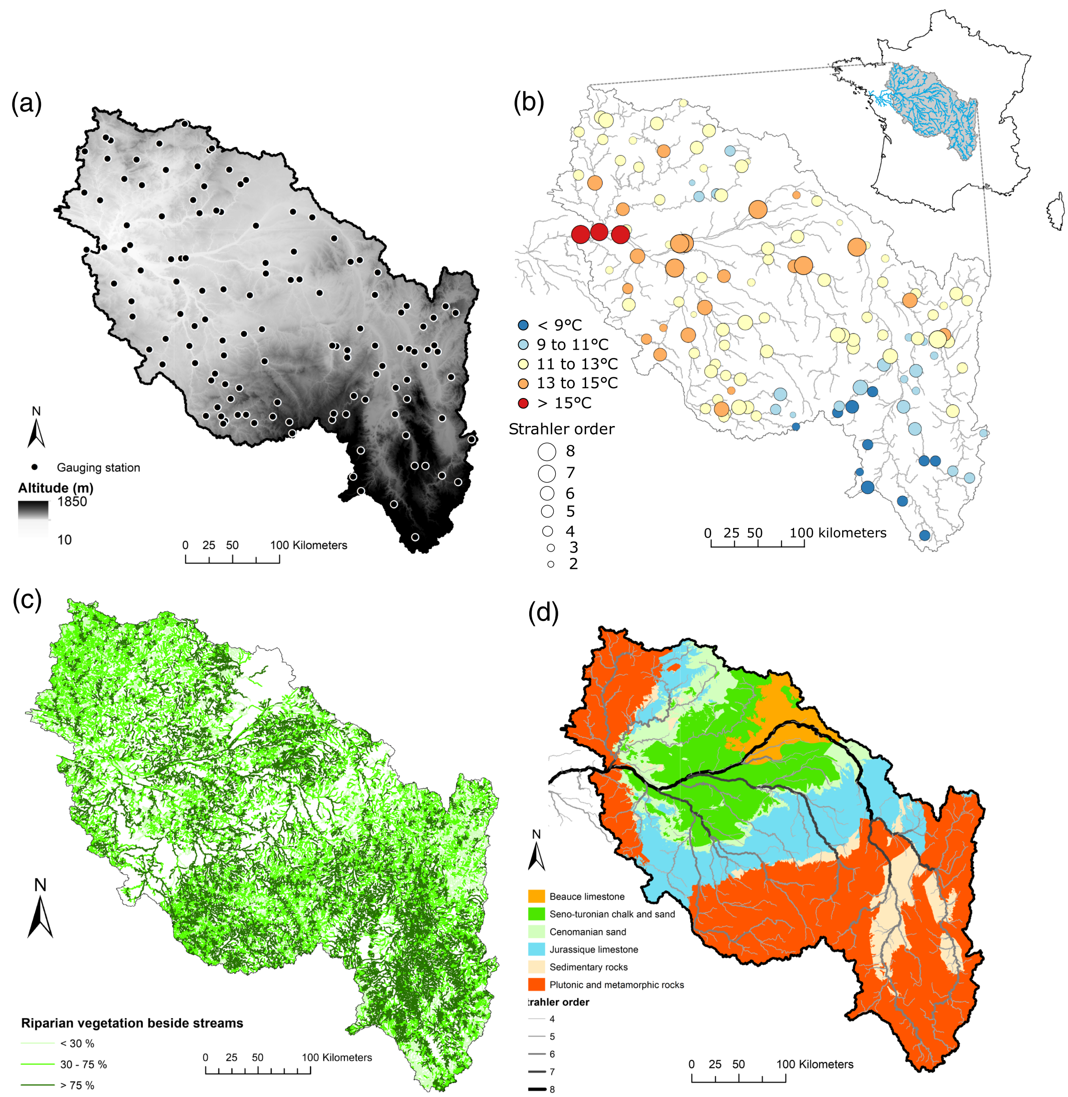

FIGURE 1 Presentation of the Loire catchment: (a) altitude and location of monitoring stations, (b) location of the 127 water temperature monitoring stations presented with the spatial distribution of mean annual stream temperatures (*TwA*), (c) vegetation cover besides streams (Valette, Piffady, Chandesris, & Souchon, 2012), and (d) main aquifer formations and basin lithology

values in time series). To limit biases in the calculation of indicators for each station, hydrological years with more than 15% of missing daily values (threshold based on previous studies (Beaufort et al., 2016; Aurélien Beaufort, Lamouroux, Pella, Datry, & Sauquet, 2018)) or with missing values during August or January are excluded from the analysis. The length of available records for the 127 stations time series varies between 1 (56 stations), 2 (29 stations), 3 (27 stations), and 4 years (15 stations).

The hourly *Ta* was taken from the SAFRAN (Système d'analyse fournissant des renseignements atmosphériques à la neige) reanalysis data (grid 8 km) at hourly time step between 2008 to 2012 (Quintana-Seguí et al., 2008; Vidal, Martin, Franchistéguy, Baillon, & Soubeyroux, 2010). *Ta* is extracted from the SAFRAN mesh (64 km^2) overlapping the station. The mean annual *Ta* of these stations ranges from 6.4°C to 12.5°C. The coldest temperatures are observed in the mountainous part of the basin (mean annual $Ta < 10$°C), whereas the warmest temperatures are observed in the west and in the sedimentary plain (mean annual $Ta > 11$°C).

Both hourly *Ta* and *Tw* have been averaged over the day and over the week in the next section.

2.2 | Metrics of air–water temperature relationship

We used four metrics to characterize the relation between air and water temperature. (a) Two of these metrics, the thermal sensitivity (*TS*) and intercept (*b*), provide information on the link between weekly *Tw* and *Ta* over the year. Weekly linear regressions were selected on the basis of the best mean R^2 fitted for the 127 stations in comparison with daily or logistic regressions.

For each station, a linear regression is fitted between the weekly *Tw* (*Tw7D*) and the weekly *Ta* (*Ta7D*) and the distribution of slopes, hereafter called thermal sensitivity (*TS*), and intercept (*b*) were analysed (Equation 1; Kelleher et al., 2012; O'Driscoll & DeWalle, 2006).

$$Tw7D = Ta7D \times TS + b. \tag{1}$$

(b) Two others metrics, ΔT_{Jan} and ΔT_{Aug}, are based on the seasonal difference between monthly *Tw* and *Ta*. For all stations, the monthly *Tw* (*MTw*) is the coldest in January and the warmest in August. To account for the relative sensitivity of *Tw* during extreme months, we introduced two metrics, which are the differences between the monthly *Ta* (*MTa*) and *Tw* in January (ΔT_{Jan}) and in August (ΔT_{Aug}) averaged between 2012 and 2016:

$$\Delta T_{\text{Jan}} = \frac{\sum_{i=1}^{i=Ny} \left(MTa_{\text{Jan}}(i) - MTw_{\text{Jan}}(i)\right)}{Ny}, \tag{2}$$

$$\Delta T_{\text{Aug}} = \frac{\sum_{i=1}^{i=Ny} \left(MTa_{\text{Aug}}(i) - MTw_{\text{Aug}}(i)\right)}{Ny}, \tag{3}$$

where ΔT is the mean difference between monthly *Ta* (*MTa*) and *Tw* (*MTw*) calculated in January or August, $MTa_{\text{Jan}}(i)$ and $MTa_{\text{Aug}}(i)$ are respectively the monthly *Ta* in January and August of the year *i*, $MTw_{\text{Jan}}(i)$ and $MTw_{\text{Aug}}(i)$ are respectively the monthly *Tw* in January and August of the year *i*, and *Ny* is the number of year where monthly *Ta* and *Tw* are both available ($1 \leq Ny \leq 4$, see Section 2.1).

2.3 | Explanatory variables

A set of eight explanatory variables was selected to explain the observed spatial pattern in *TS* and identify main drivers of thermal streams moderation. The variable selection was based on the most pertinent variables identified in literature and on the results of a principal component analysis (not presented here) to minimize dependency between variables.

The distance from the source (*D* in km) and the elevation (*E* in m) are determined at the location of each monitoring station. The slope of the river reach (*S* in m m^{-1}) where the station is located is determined with BD ALTI® 25-m resolution DTM dataset (IGN Paris, France). A higher *S* increases the flow velocity, and *E* influences *Tw* through the association with the adiabatic lapse rates of *Ta* and also through snow and glacier meltwater inflow, which should cool *Tw* at higher elevations. Streams with a high *D* have more time to equilibrate their *Tw* with *Ta*.

Two hydrological indicators were also introduced. (a) The baseflow index (*BFI*) was estimated with the method of the Institute of Hydrology (1980) between 2008 and 2012. The BFI is a measure of the proportion of the low-flow component to the total river flow with values between 0 and 1. Details on calculation can be found in Gustard, Bullock, and Dixon (1992). Low values are related to catchments with no storage capacity and also to catchments exposed to very high climate variability resulting in severe low-flow and quick run-off in response to rainfall events. High values are observed where artificial reservoirs, large aquifers, and storage in snow packs moderate the variability of daily flow. In our study, *BFI* is considered as a proxy of groundwater influence. The discharge *Q* was not monitored at *Tw* station, and each *Tw* station was coupled to the nearest gauging station (distance between both stations ranges from 10 m to 15 km). The matching is based on two criteria: (a) The gauging stations has to be located in the same or nearby streams and (b) the difference of catchment area between the location where *Tw* was measured and the location where *Q* was measured was kept to a maximum of ±20%. The daily discharge was extracted from the French river flow monitoring network (HYDRO database, http://www.hydro. eaufrance.fr/). (b) The average specific discharge in August (Q_{Aug}) is calculated at each station between 2008 and 2012. The goal is to measure the capacity of the catchment to produce a flow in summer, when precipitation is low. The specific discharge is the ratio between the discharge and the corresponding catchment area (in L s^{-1} km^{-2}) and is used to standardize discharge for basin area.

Two climatic variables were determined from the Safran reanalysis data: (a) the mean summer cumulated precipitation (*P* in mm) and (b) the mean summer potential evapotranspiration (*PET* in mm) both calculated between June 1 and September 30 of each year between 2008 and 2012 for the entire upstream area of each monitoring station. Streams with wetter basin (high *P* and low *PET*) are expected to have higher water yields and more groundwater contributions that should cool streams (Isaak et al., 2017).

One variable was determined to characterize the riparian vegetation. A shading factor (*SF*), corresponding to a coefficient of reduction of the overall incident radiation, was estimated by Valette et al. (2012). *SF* gives the averaged vegetation cover (%) derived from a buffer of 10 m of vegetation polygons on both sides of reaches from the BD TOPO® database, provided by Institut national de l'information géographique et forestière (IGN). *SF* has been calculated between 7 a.m. and 9 p.m. over the summer period between June 1 and September 30 over the period 2008–2012, when the effect of shading is at its annual seasonal maximum for the North Hemisphere. The model of Li, Jackson, and Kraseski (2012) was implemented in its simplest version, that is, considering rectangular trees, located at the edge of the bank, without overhang.

$$SF = \frac{H \times \cot \Psi \times \sin \delta}{W} \times vc, \tag{4}$$

where H is the tree height (assumed to be 20 m everywhere), W is the stream width, estimated using the ESTIMKART empirical model (Lamouroux et al., 2010), Ψ is the solar elevation angle, δ is the angle between solar azimuth and the mean azimuth (0–180°) of the river reach, and vc is the vegetation cover (%).

2.4 | Statistical classification and explanatory variables

2.4.1 | Thermal regimes clustering

To identify natural thermal regimes of stations sharing similar *Ta*–*Tw* relationship, an agglomerative hierarchical clustering (AHC) has been used. The AHC is based on the four metrics described above (*TS*, *b*, ΔT_{Jan}, and ΔT_{Aug}). The Euclidean distance is used to measure the dissimilarity, and clusters are found with the Ward's minimum variance method. The stability of clusters is assessed through a bootstrap approach with the R package "fpc" (Hennig, 2019), and the similarity between each new cluster set and initial cluster was assessed with the Jaccard index (Hennig, 2007; Maheu et al., 2016). The Jaccard coefficient ranges from 0 to 1, and a cluster with a coefficient larger than 0.75 can be considered as stable (Maheu et al., 2016). Each thermal regime identified is described in terms of magnitude (mean *Tw* over a month) and amplitude (differences between the maximum and minimum values of *MTw*) and compared with *MTa*.

2.4.2 | Identification of environmental drivers in thermal sensitivity

A CART is used to examine the relationship between *TS* and the set of explanatory variables described above. CART analysis (Breiman, Friedman, Stone, & Olshen, 1984) is nonparametric and non-linear and does not introduce an a priori structure of the link between explanatory variables and the variable to be explained contrary to generalized linear models implicit assumption (Breiman et al., 1984; Ripley, 1996). CART recursively partitions observations in a matched data set, consisting of *TS* (response) and the eight explanatory variables, into progressively smaller groups (De'ath & Fabricius, 2000). Each partition is a binary split. During each recursion, splits for each explanatory variable are examined, and the split that leads to the most homogeneous subgroups with respect to the dependent variable is chosen. The interpretation of results summarized in a tree with series of logical if-then conditions (tree nodes) is very simple. We used the R package "rpart" (Version 4.1, Therneau & Atkinson, 2018) for implementing the CART model. The random forest (RF) model was used to assess the importance of explanatory variables for the prediction of *TS* and to evaluate the robustness of the classification. RF combines decision trees obtained by resampling the calibration set (Breiman, 2001), which is constituted by selecting randomly 80% of the observations (80% of 127 stations × eight explanatory variables × *TS*), and the test set consists of the remaining 20%. We used the implementation in the R package "randomForest" (Liaw & Wiener, 2002). The explanatory variable importance is given directly by the "randomForest" algorithm, which determines how much the mean square errors in prediction increases when that covariate is randomly permuted within the tree. The random selection is performed 100 times, and the explanatory variables importance for each test set was then averaged.

3 | RESULTS

3.1 | Distribution of thermal sensitivity and link with catchment size

The R^2 values for weekly *Ta* and *Tw* ranged from.83 to.98, with values greater than.9 at 123 of the 127 sites. *TS* ranges from 0.42 (Figure 2b) to 1.2 (Figure 2a), and *b* ranges from 0.5°C to 7.5°C. Regression lines plotted for the 127 stations showed a higher range of values of *Tw* when *Ta* is high at the regional scale (*Tw* ranges between 15°C and 30°C when *Ta* is 25°C) than when *Ta* is low (*Tw* ranges between 0°C and 7.5°C when *Ta* is 0°C; Figure 2c).

The relationship between *TS* and *b* shows a moderate negative correlation with $R^2 \approx 0.7$. Stations with the lowest *TS* (<0.6) and the highest *b* have the highest residual and seemed to follow a different pattern than other stations (Figure 3a; all the points are located above the regression line). Stations having a moderate *TS* between 0.6 and 0.9 are most often observed across the Loire River basin, and their associated *b* ranges from 1°C to 5°C. Stations with a high *TS* (>0.9) and a small *b* (<3) follow the same trend and have small residuals of the slope intercept regression. The analysis of weekly *Ta*–*Tw* relationship indicates that *TS* generally increases with stream size and the distance from source (Figure 3b). Streams with a distance from source higher than 100 km^2 obtain a *TS* higher than 0.7. For small and medium rivers (D < 100 km), the range of *TS* is large and between 0.42 and 1.

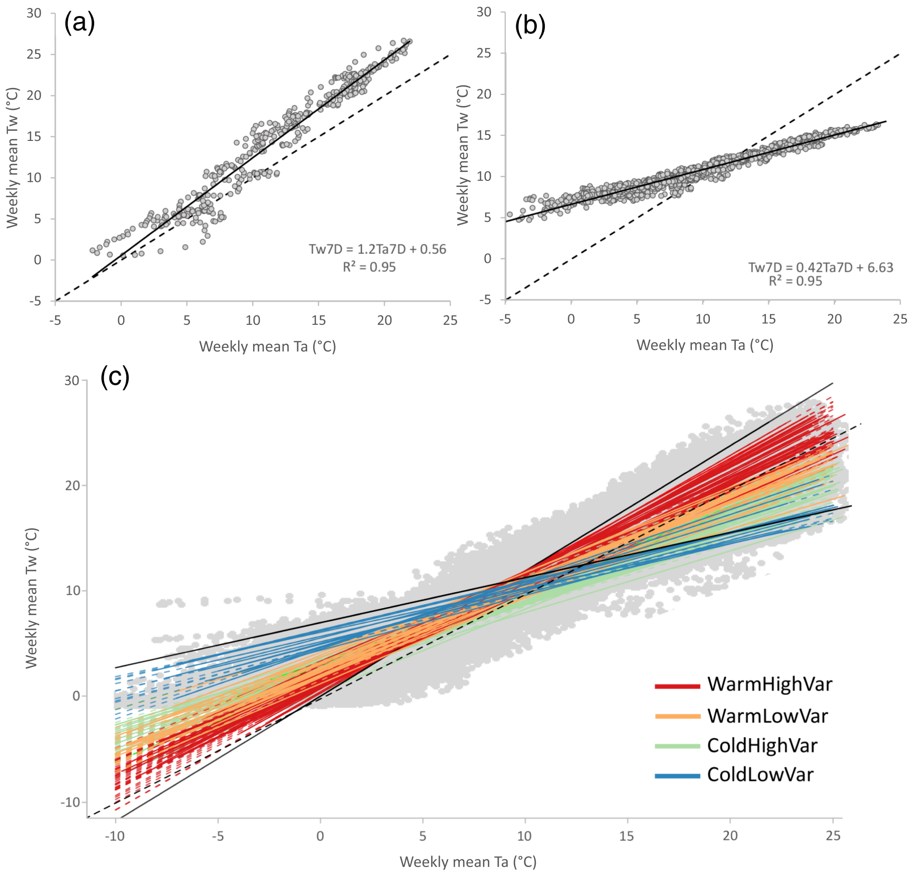

FIGURE 2 *Tw*–*Ta* weekly linear regression: (a) for the station with the highest *TS*, (b) for the station with the lowest *TS*, and (c) for the 127 stations fitted on data available between 2008 and 2012. Dashed lines represent the curve *x* = *y*, solid lines represent the weekly linear regression curves for each station, and the black solid lines in (c) correspond to weekly linear regression curves of stations represented in (a) and (b), and grey points in (c) represents all the observations

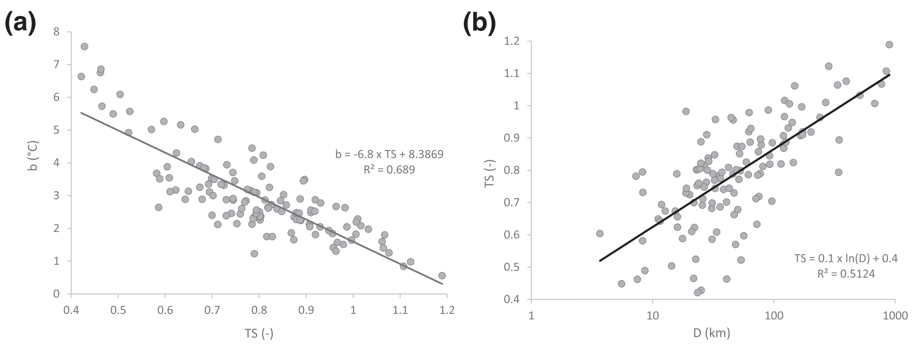

FIGURE 3 Distribution of *TS*: (a) relationship between *b* and *TS* of weekly *Tw*–*Ta* linear regressions and (b) *TS* as a function of the distance from the source (*D*) of monitoring stations

The analysis of the spatial distribution of *TS* in the Loire basin shows that the stations obtaining the smallest *TS* (*TS* < 0.5) are located in the sedimentary plain where the main aquifer formations are located (Figure 4). The stations with the highest *TS* (*TS* > 0.9) are located along large rivers in the sedimentary plain and in the western side of the basin where the altitudes are the lowest and *Ta* the highest. Finally, stations located in the regions with the highest altitude obtain a moderate *TS* lower than 0.7.

3.2 | Cluster classification analysis

The AHC yielded four clusters of station corresponding to four thermal regimes:

- WarmHighVar—warm and high variability (47 sites—37%): stations characterized by low *b* (<3°C) and high *TS* (>0.8). At these stations, *MTw* is higher than *MTa* in January and August with a median difference of 1.5°C (Table 1). These stations are those with the highest annual amplitude of *MTw* reaching 18°C with similar annual *MTa* amplitude (red area; Figure 5a,b). Their *MTw*s are the warmest during summer and exceed 21°C on average.
- WarmLowVar—warm and low variability (23 sites—18%): These stations are characterized by a smaller *TS* and a higher *b* (median *b* = 3.5°C) than stations from WarmHighVar. *MTa* is less than *MTw* in winter with a median deviation of 3°C. In August, the *MTw* is very close to *MTa*, and ΔT_{Aug} does not exceed 1°C. They have annual *MTw* amplitude of 14°C and *MTw* smaller than 4°C in

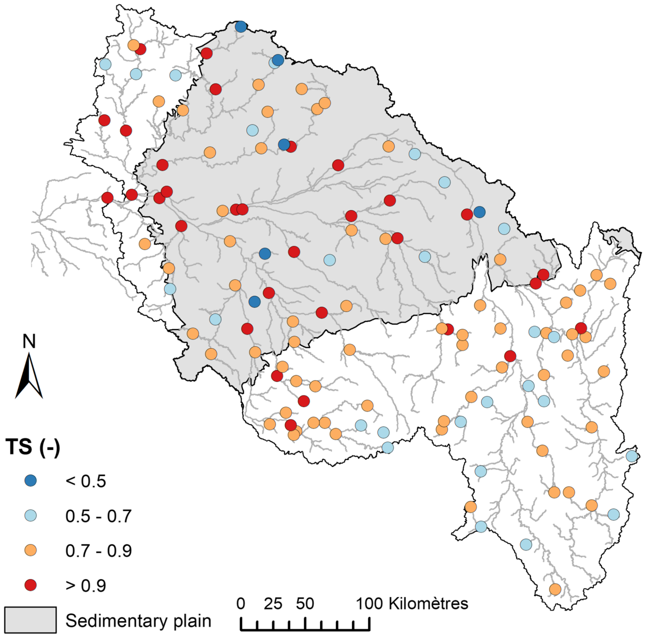

FIGURE 4 Spatial distribution of *TS* calculated between 2012 and 2016 on weekly *Ta*–*Tw* regressions

summer in comparison with the *MTw* of stations from WarmHighVar (yellow area; Figure 5a,b).

- ColdHighVar—cold and high variability (44 sites—35%): Stations have *MTw* higher than *MTa* in January by 2°C (Table 1). Inversely, in August, *MTw* is less than *MTa* by 2°C. The *TS* and *b* of stations have rather average values with medians of 0.7 and 2.9, respectively. They have annual *MTw* amplitude of 14°C and *MTw* less than 5°C in summer in comparison with the *MTw* of stations from WarmHighVar (green area; Figure 5a,b).
- ColdLowVar—cold and low variability (13 sites—10%): Stations demonstrate the lowest *TS* of each class (*TS* < 0.7) and the highest *b* (greater than 4.9°C). The differences between *MTw* and *MTa* are high, in comparison with other thermal regimes, whether in August (*MTa* > *MTw* by 3.5°C) or in January (*MTa* < *MTw* by 4°C). These stations are those with the lowest annual *MTw* amplitude of 9°C, which is one half less than the amplitude of stations from WarmHighVar (blue area; Figure 5a). The *MTw* of stations from ColdLowVar is the lowest during summer (*MTw* = 15°C) and the warmest during winter in comparison with others thermal regimes (Figure 5c).

The thermal regimes named "WarmHighVar" and "ColdLowVar" were stable clusters and had a Jaccard coefficient larger than 0.7. The thermal regimes called "WarmLowVar" and "ColdHighVar" were less stable clusters and had Jaccard coefficients of 0.55 and 0.61, respectively. The analysis of the deviation from the mean annual *Tw* (*MTw*) and of *MTw* averaged over the four clusters identified by AHC led to distinguish significantly different thermal regime in terms of magnitude and amplitudes (Figure 5a,c) in comparison with *MTa* (Figure 5b,d).

The *MTa* patterns of each cluster demonstrate a very similar amplitude and magnitude (Figure 5b,d) with annual amplitude close to 18°C following the same amplitude of thermal regime WarmHighVar. The different response of each thermal regime to same climate conditions suggests other controlling factors than climate determine the annual amplitude and magnitude of *Tw*.

3.3 | Drivers of thermal sensitivity (*TS*)

The CART model output leads to develop dichotomic tree plots to better visualize the effects of main drivers (Figure 7). The three most important explanatory variables used by the model to cluster stations as a function of their *TS* are *SF*, *D* (distance from source), and *BFI* (Figure 6). This is consistent with the RF model output where *D*, *SF*, and *BFI* are identified as the main environmental variables to explain the *TS* of streams (variable importance >15%; Figure 6). The variables Q_{Aug} and *S* are also used to differentiate clusters in the CART model and obtained a moderate importance close to 8% with RF. Elevation (*E*) is identified as the fourth relevant variable with RF model (variable importance = 11%; Figure 6) but is not used by the CART model for

TABLE 1 Metrics averaged for each thermal regime determined with the agglomerative hierarchical clustering

Cluster		TS	b	ΔT_{Jan}	ΔT_{Aug}
WarmHighVar—warm and high variability 47 sites—37%	Max	1.2	3.5	−0.4	1.1
	Med	0.9	2.2	−1.4	−1.6
	Min	0.8	0.6	−2.7	−4.2
WarmLowVar—warm and low variability 23 sites—18%	Max	0.8	4.7	−1.7	1.0
	Med	0.8	3.5	−3.1	−0.3
	Min	0.7	2.5	−4.0	−1.1
ColdHighVar—cold and high variability 44 sites—35%	Max	0.8	4.3	−0.8	5.8
	Med	0.7	2.9	−1.8	1.9
	Min	0.6	1.2	−4.1	0.7
ColdLowVar—cold and low variability 13 sites—10%	Max	0.7	7.6	−2.9	4.7
	Med	0.5	5.7	−4.0	3.5
	Min	0.4	4.9	−5.7	1.1

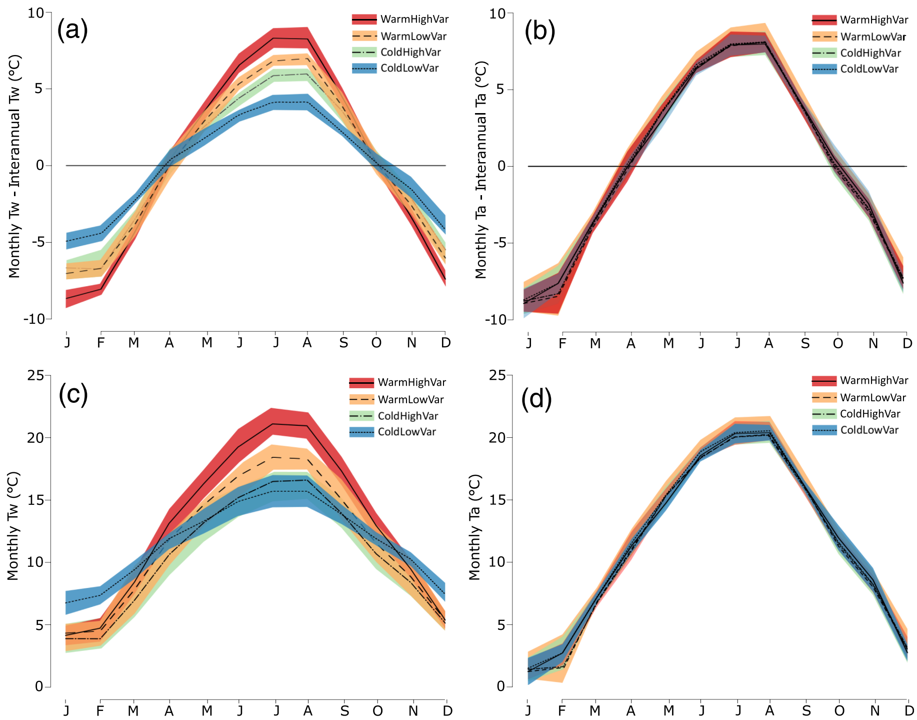

FIGURE 5 Representation of (a) the deviation from the mean annual *Tw*, (b) the deviation from the mean annual *Ta*, (c) the monthly *Tw*, and (d) the monthly *Ta* averaged over the four thermal regimes identified by agglomerative hierarchical clustering. The colour area bars represent ± standard deviation of each series

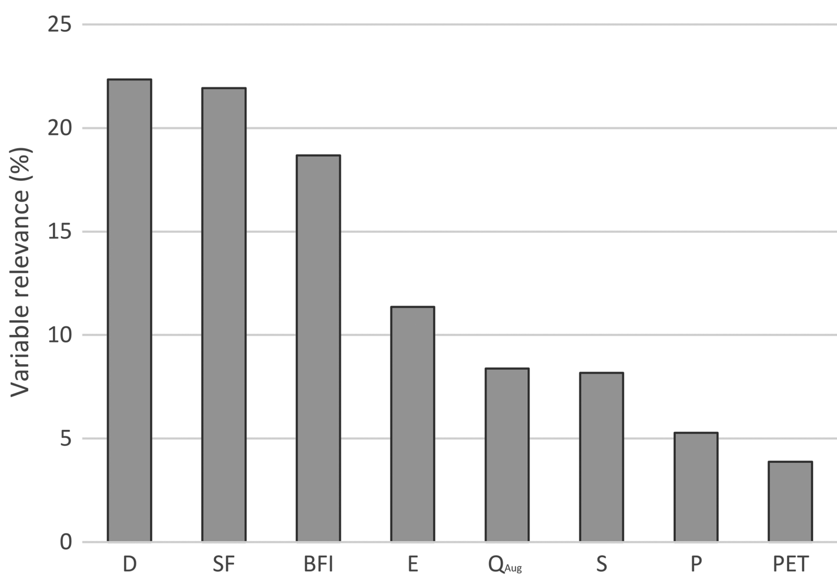

FIGURE 6 Variable importance to explain *TS* for all stations ranking from the highest to the lowest obtained from random forest

stations clustering. Others variables have a lower influence on *TS* and are not used in the dichotomic tree plot from the CART model.

- C1—low *TS* with high *SF* and high *BFI*: The combined effect of a high *SF* (*SF* > 30%) and a high *BFI* (*BFI* > 0.8) led to strongly reduce *TS* of streams (mean *TS* of 0.5; Figure 7). The 11 stations having these characteristics belong to the thermal regime ColdLowVar (Table 2).
- C2 and C3—low and moderate *TS* with high *SF*: Streams with an *SF* higher than 30% and a *BFI* less than 0.8 belong mostly to the thermal regime ColdHighVar from AHC results (Figure 7). Q_{Aug} has also an important influence, and we can see contrasts in terms of *TS* within this class. The *TS* was lower for the 17 stations located on streams with a Q_{Aug} value higher than 5 L s^{-1} km^{-2} (mean *TS* = 0.67; C2) than for the 29 remaining stations in C3 with a Q_{Aug} value less than 5 L s^{-1} km^{-2} (mean *TS* = 0.76).
- C4—moderate *TS* with low *SF*, low *D*, and high *BFI*: The six stations with *SF* less than 30%, a *D* less than 120 km, and a *BFI* greater than 0.8 have a moderate *TS* (mean *TS* of 0.71, C4) and belong to the two thermal regimes WarmLowVar and ColdLowVar (Table 2).
- C5 and C6—moderate and high *TS* with low *SF*, low *D*, and low *BFI*: Stations located on small and medium streams (*S* < 120 km) with a *BFI* lower than 0.8 obtained moderate and high *TS*. The *TS* of the 13 stations located on streams with a higher slope (*S* > 2.5 m km^{-1})

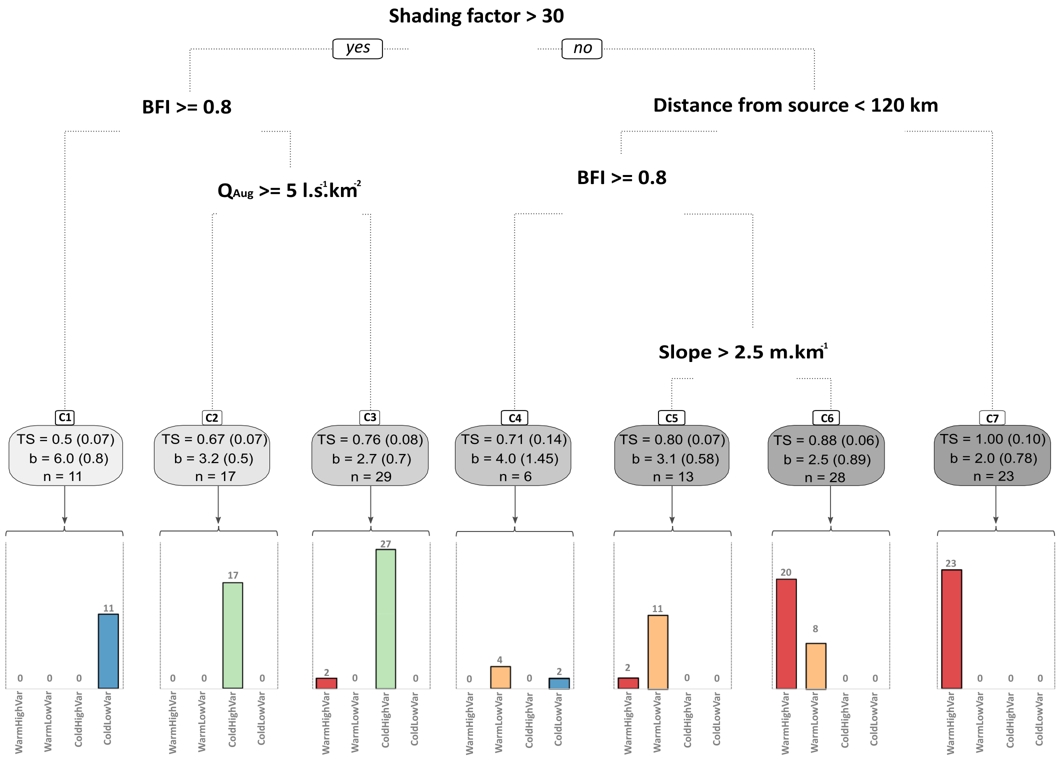

FIGURE 7 Regression and classification on tree developed for *TS* for all explanatory variables. In each cluster, the mean *TS*, the mean *b*, their standard deviation on (in brackets), and the number of stations (*n*) are presented. Histograms under each branch indicate the thermal regimes of stations identified by the agglomerative hierarchical clustering analysis

TABLE 2 Explanatory variables presented for each thermal regime identify with the agglomerative hierarchical clustering

Cluster		OS	D (km)	E (m)	S (m km^{-1})	SF (%)	BFI (–)	Q_{Aug} (L s^{-1} km^{-2})	P (mm)	PET (mm)
WarmHighVar	Max	8	896	323	12.6	60	0.81	1.1	294.0	308.7
	Med	5	122	101	0.5	20	0.72	2	211.2	283.1
	Min	3	19	10	0.1	0	0.51	0.3	144.5	258.6
WarmLowVar	Max	5	145	1120	29.7	29	0.95	3.7	352.2	313.1
	Med	4	36	282	3.3	15	0.74	3	214.0	284.9
	Min	2	7	88	0.1	0	0.64	0.2	140.9	261.0
ColdHighVar	Max	6	96	755	26.1	77	0.78	9.9	302.9	313.5
	Med	4	26	232	3.3	50	0.71	4	231.3	281.8
	Min	2	4	41	0.1	30	0.49	0.1	151.4	256.4
ColdLowVar	Max	5	73	231	3.8	71	0.92	1.7	237.1	312.6
	Med	3	24	122	1.5	50	0.86	5	188.0	283.2
	Min	2	6	65	0.1	19	0.81	0.5	148.0	248.6

have a lower sensitivity (mean *TS* of 0.81; C5) in comparison with the 28 remaining stations from C6 (mean *TS* of 0.88; C6). The 13 stations in C5 mostly belong to the thermal regime WarmLowVar, whereas the 28 stations in C6 mostly belong to the thermal regime WarmHighVar (Table 2).

- C7—high *TS* with low *SF*, low *D*, and high *BFI*: Stations located on streams with low *SF* (*SF* < 30%) and a high *D* (*D* > 120 km) have the highest *TS* (mean *TS* of 1; C7; Figure 7). The 23 stations having these characteristics belong to the thermal regime WarmHighVar (Table 2).

4 | DISCUSSION

4.1 | Regression robustness and comparison with other studies

In our case study, best correlations between *Ta* and *Tw* were obtained with linear regression models and at the weekly time step, with a mean R^2 of 0.96 (standard deviation [*SD*] = 0.02) determined for the 127 stations. Weekly *Ta*–*Tw* linear regressions slightly outperform daily *Ta*–*Tw* linear regressions (mean R^2 = 0.88; *SD* = 0.03) as well as daily (mean R^2 = 0.86; SD = 0.05) and weekly (mean R^2 = 0.93; SD = 0.03) logistic regressions. The weekly time step is more accurate because this time step filters out the lag time between *Ta* and *Tw* peaks, which can be of several days. In contrast to other studies (e.g., Kelleher et al., 2012), taking into account a non-linear relationship between *Ta* and *Tw* did not improve the performance of the regressions. This is probably explained by the fact that the Loire basin is not subject to *Ta* (min weekly *Ta* across the Loire basin between 2008 and 2012 = −8°C) as low as in cold, continental regions studied in the contiguous United States (min *Ta* = −20°C; Omid Mohseni, Stefan, & Erickson, 1998; Kelleher et al., 2012), which makes *Ta*–*Tw* relationship more non-linear for low values. In comparison with the studies using weekly *Ta*–*Tw* linear regressions, the R^2 values calculated on the 127 stations are on average higher (mean R^2 = 0.96) and comparable with the results of Webb (1992) and O'Driscoll and DeWalle (2006). The negative correlation between *TS* and *b* is also consistent with previous studies. Streams controlled by groundwater inflows are characterized by intercepts closer to the regional groundwater temperature and low slopes. Inversely, streams more sensitive to climate conditions have steeper slopes and lower intercepts closest to *Ta*.

Our *TS* and *b* range were consistent with other studies results for linear regression models using a weekly time scale (Table 3). These *TS* and *b* values were close to those found by Webb (1992), Stefan and Preud'homme (1993), and Morrill et al. (2005) except that we observe no negative *b* and the range of our *TS* and *b* is slightly higher (Figure 8). This can be explained by a higher number of streams used in our study and by the larger size of the watershed compared with other studies (Table 3). O'Driscoll and DeWalle (2006), Kelleher et al. (2012), and Krider et al. (2013) obtained lower values of *TS* and higher *b* values for their studied streams located in karst basins.

4.2 | Groundwater influence on *TS*

In theory, groundwater influence is more visible on smaller streams because the volume of water is small and the travel time of the water from the source is short and not sufficient to equilibrate *Tw* with the atmosphere (Beaufort et al., 2016; Mohseni & Stefan, 1999). Groundwater inflow is a heat source during winter and a heat sink during summer resulting in little seasonal variation in *Tw* and a low *TS* (Hannah, Malcolm, Soulsby, & Youngson, 2004; Kelleher et al., 2012). Stations with a thermal regime ColdLowVar have low *TS* (median *TS* = 0.5) and a high intercept (median *b* = 5.7°C). In other studies, low *TS* could be due to the upstream influence of reservoirs or impoundments (Erickson & Stefan, 2000; Morrill et al., 2005) or to high groundwater contribution (Kelleher et al., 2012). The 13 stations from the thermal regime ColdLowVar have a reduced annual variation of *Tw* (blue area; Figure 5a), and their low *TS* could be reasonably related to the groundwater inflows that decrease *Tw* response to changes in *Ta* and increase the thermal inertia of streams (O'Driscoll & DeWalle, 2004). This statement is reinforced by their location on small streams above the main aquifer formations (Figure 4).

CART model results showed that all stations of the thermal regime ColdLowVar have *BFI* greater than 0.8, which seems to confirm

TABLE 3 *TS*, *b*, and R^2 values found in reviewed publications for linear regression models of weekly *Ta*–*Tw* relationship

Study	Location	TS slope	b intercept	R^2	Length of record	Koppen–Geiger climate designation
Webb (1992)	36 streams in the United Kingdom	0.65 to 1.16 (1.00)	−0.3 to 3.7 (1.0)	0.86 to 0.97 (0.91)		Cfb
Stefan and Preud'homme (1993)	11 rivers located in the Mississippi River (USA), 150,000 km^2	0.67 to 1.02 (0.86)	0.4 to 5.4 (2.9)	0.75 to 0.97 (0.89)	1 to 8 years	Cfa/Dfa
Pilgrim, Fang, and Stefan (1998)	39 streams in Minnesota (USA)	0.71 to 1.15 (0.99)	−1.5 to 4.8 (1.7)	0.67 to 0.96 (0.85)	1 to 32 years	Dfa/Dfb
Morrill, Bales, and Conklin (2005)	43 U.S. and international streams, 50,000 km^2	0.35 to 1.09 (−)	0.46 to 5.80 (−)	0.42 to 0.83 (−)	1 to 6 years	Cfa/Cfb/Dfa/Dfb
O'Driscoll and DeWalle (2006)	12 streams in Pennsylvania (USA), 450 km^2	0.18 to 0.67 (0.47)	3.2 to 9.1 (6.1)	0.86 to 0.97	3 years	Dfa/Dfb/Cfa
Kelleher et al. (2012)	57 streams in Pennsylvania (USA), 17,500 km^2	0.01 to 1.05 (−)	—	0.09 to 0.98 (−)	2 years or greater	Dfa/Dfb/Cfa
Chang and Psaris (2013)	74 streams in Columbia River basin (USA)	0.10 to 0.81	—	>0.7	—	Csb/Dsb/BWk/Cfb/Dfb
Krider, Magner, Perry, Vondracek, and Ferrington (2013)	40 streams in Minnesota (USA), 7,200 km^2	0.18 to 0.74 (0.3)	2.9 to 8.3 (6.65)	0.59 to 0.98 (0.89)	1 to 4 years	Dfa/Dfb
Present study	127 streams in the Loire basin, 110,000 km^2	0.42 to 1.19 (0.79)	0.6 to 7.5 (3.0)	0.83 to 0.98 (0.95)	1 to 4 years	Cfb

Note. The value in brackets corresponds to the average value.

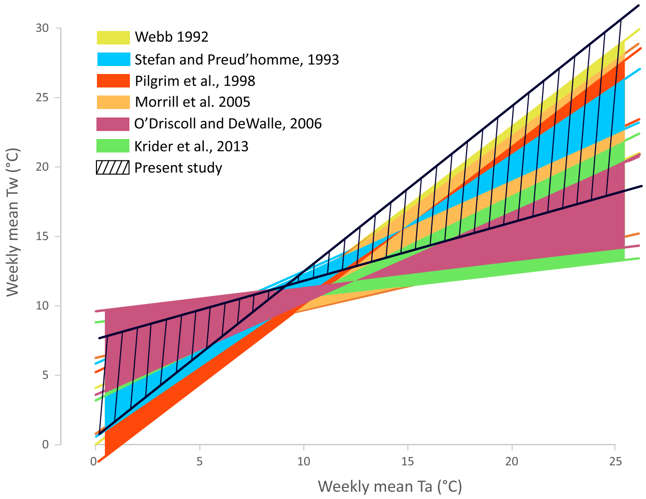

FIGURE 8 Representation of the range of *TS* and *b* found in reviewed publications for linear regression models of weekly *Ta*–*Tw* relationship

groundwater influences (C1 and C4; Figure 7). The decrease of *TS* is accentuated when a high *BFI* is combined with an *SF* higher than 30% as on the 11 stations in C1 (mean *TS* = 0.5). The shading of riparian vegetation leads to increase the thermal moderation of surface water in summer by shading from solar radiation. The *BFI* appears as a very influential variable in *TS* (Figure 6). However, in the Loire basin, *TS* remains greater than 0.4 even when the *BFI* is higher than 0.8 and when *b* is higher than 6°C. In other studies, *TS* values are close to 0 when the *BFI* is close to 1 (Kelleher et al., 2012). It could be suspected that the temperature of groundwater inflows feeding streams follows a seasonal trend correlated with *Ta* and more marked than those observed in the literature (Kelleher et al., 2012; Krider et al., 2013; O'Driscoll & DeWalle, 2006). This could also explain the high residuals of slope intercept regression for stations having a *TS* lower than 0.6 (Figure 3a).

The variable Q_{Aug} is the mean specific discharge during the warmest month and represents the sustainability of low flows. It is a moderately influential variable in *TS* (Figure 6). It can be assumed that a stream with a high Q_{Aug}, in the case of natural flowing, benefits from groundwater inflows and/or of important contribution of its tributaries allowing it to maintain a sufficient depth to moderate *Tw* in summer. CART analysis results showed that streams with a Q_{Aug} value higher than 5 L s^{-1} km^{-2}, associated to an *SF* less than 30% and a *BFI* less than 0.8, have a lower *TS* than others stations (C2 vs. C3; Figure 7), which seems to confirm our assumption. However, the importance of Q_{Aug} remains applies to a subset of stations and the *BFI* remains the main variable representing the influence of groundwater inflows in our dataset.

4.3 | Riparian shading influence on *TS*

Shortwave (solar) radiation is one of the most influential factors that influence stream temperature and is related directly to the amount of shading provided by riparian vegetation (O'Driscoll & DeWalle, 2006; Sinokrot & Stefan, 1993). The riparian vegetation captures solar radiation and leads to reduced *Tw* resulting in a decrease of *TS*. This effect is particularly visible in summer when the solar radiation is the strongest and represents the main source of energy inputs (e.g., Hannah, Malcolm, Soulsby, & Youngson, 2008). In addition, the riparian vegetation of the Loire basin is mainly composed of deciduous trees, which considerably limit the effect of shading in winter. The influence of the riparian vegetation shading on *TS* was highlighted by several studies (Chang & Psaris, 2013; Dugdale et al., 2018; Garner, Malcolm, et al., 2017; Hrachowitz et al., 2010; F.L. Jackson et al., 2017; Loicq et al., 2018). However, it is still complex to characterize the own effect of riparian shading, and shading effect is regularly lumped to other drivers of *TS* moderation (Kelleher et al., 2012; O'Driscoll & DeWalle, 2006).

In our study, we tried to differentiate the effects of shading and of groundwater inflows. The only study of *TS* and *b* does not allow to clearly make this distinction because the effect of riparian vegetation shading could be mixed with the effect of groundwater inflows. The ΔT_{Jan} and ΔT_{Aug} were introduced in the AHC model to help make this distinction. Stations in thermal regime WarmHighVar have a high *TS* (*TS* > 0.8) combined to a small intercept (*b* < 3.5°C) and are supposed the most influenced by climate and *Ta*. Their amplitude and magnitude of *MTa* and *MTw* are very similar and follow the same trend (amplitude of 18°C; Figure 5a) and do not seem to be moderated by any drivers. Stations in thermal regime ColdHighVar have a lower *TS* (*TS* < 0.8) and slightly higher intercept (median *b* = 2.9°C) than in thermal regime WarmHighVar (Table 1). Between thermal regimes ColdHighVar and WarmHighVar, their ΔT_{Jan} is similar (ΔT_{Jan} = −1.6°C), but *Tw* is clearly lower than *Ta* during August for stations in thermal regime ColdHighVar (median ΔT_{Aug} = 1.9). The influence of the riparian vegetation shading is suspected. CART model results seems to confirm this assumption because all stations in ColdHighVar were identified with an *SF* higher than 30% (C2 and C4; Figure 7). The effects of shading could be accentuated when the specific discharge in August is higher than 5 L s^{-1} km^{-2} (C2; *TS* ≈ 0.67) because the thermal inertia of the streams is increased.

4.4 | Landscape factors influence

The distance from the source (*D*) is a key driver of *TS* (Figure 6). CART model results showed that stations with a *D* higher than 120 km obtained the highest *TS* (*TS* = 1; C7; Figure 7). *D* is highly positively correlated with the drainage area, and several studies identified this driver as playing an important role in the *TS* of rivers (Chang & Psaris, 2013; Garner et al., 2014; Hrachowitz et al., 2010; Imholt et al., 2013). Some others studies have also identified the Strahler order, which is correlated to *D* (R^2 = 0.6), as a strong influence factor of *TS* (Chang & Psaris, 2013; Ducharne, 2008; Kelleher et al., 2012; Wehrly, Wiley, & Seelbach, 1998). Streams with a high *D* and a large drainage area are weakly dependent on upstream conditions, and the travel time of the water body between upstream and downstream allows *Tw* to equilibrate with *Ta* (Mohseni & Stefan, 1999), leading to increase *TS*. Also, a longer *D* and a larger catchment area corresponds to lower topographical slopes, slower flow velocities, and greater regional residence time, which allow more time for *Tw* to adjust to local *Ta* (Mayer, 2012).

Stations located on small and medium streams, not influenced by shading and groundwater inflows (*SF* < 30%; *BFI* < 0.8; and *D* < 120 km) belonging to cluster C5 and C6 (Figure 7), obtained a *TS* less than those of large rivers in C7. There is an influence of *S* because stations located on streams with a high slope (S < 2.5 m km^{-1}) had a mean *TS* of 0.8 (C5; Figure 7), whereas others had a mean *TS* of 0.88 (Cluster C6; Figure 7). The stream slope is mostly linked to elevation (R^2 = 0.65). A higher slope increases the flow velocity, and the elevation influences *Tw* over the adiabatic lapse rates of *Ta* (Hrachowitz et al., 2010) and also through snow and glacier meltwater inflow (Arora, Toffolon, Tockner, & Venohr, 2018; Morrill et al., 2005), which may contribute to decrease *TS*. *P* and *PET* are not relevant in CART model, which may be explained by the relative climatic homogeneity of the study area (Cfb = temperate oceanic climate, Table 3).

4.5 | Implication for river management and river restoration

The study of streams *TS* makes it possible to identify the most sensitive streams to environmental change (high *TS*) and potentially the most sensitive to the effects of climate change. The stationarity of all processes influencing *Tw* is difficult to estimate because it implies the use of physically based models directly integrating energy fluxes because the only study of *TS* tends to underestimate the warming of climate change (Leach & Moore, 2019). However, streams studied here have a natural thermal regime and are not influenced by anthropogenic activities. These natural streams sensitive to environmental changes in the present time (high *TS*) will always be sensitive to environmental changes in the future without human actions. The goal of our approach is to identify the most climate-sensitive streams, linking them to environmental or hydrological features, to guide stakeholders to pay particular attention to them.

Our analysis identified *D*, *BFI*, and *SF* as the main factors influencing *TS* in the Loire basin. The major streams of the Loire catchment (*D* > 120 km) show the highest *TS* value (mean *TS* = 1) and appear highly sensitive to the effects of global warming. For these streams having a large wet width (>50 m), the effects of shading from riparian vegetation are very small, and actions to reduce *TS* are limited. Thermal anomalies could be detected by aerial infrared survey (Wawrzyniak, Piégay, & Poirel, 2012) and be preserved by limiting advective thermal mixing (Kurylyk et al., 2015) or activated by geomorphological restoration of streams (Eschbach et al., 2017; Loheide & Gorelick, 2006). On small and medium streams, it is necessary to preserve and/or favour the presence of riparian vegetation to moderate *TS* (Fabris, Malcolm, Buddendorf, & Soulsby, 2018). The effects will be most pronounced, in comparison with large streams, because of their smaller width, but investments have to be made strategically (Isaak et al., 2017; Johnson & Wilby, 2015). From a watershed management perspective, stream shading would be less effective in streams where *Tw* is already strongly moderated by groundwater inflows but more effective along losing reaches or stream reaches distant from groundwater inflows (O'Driscoll & DeWalle, 2006).

Streams with a low *TS* have a limited surface water heating during summer and may provide thermal refuges for thermo-sensitive aquatic species (macroinvertebrates, stream-dwelling amphibians, and fish species; Isaak et al., 2017). In order to limit these warmings and preserve ecosystems, it seems important to identify streams constituting cold-water thermal refuges (with low *TS*) and to restore and preserve thermal diversity in the hydrographical network (Torgersen, Ebersole, & Keenan, 2012). However, the main factors limiting *TS* (*BFI* and *SF*) could change in the future, and several streams could become much more sensitive to environmental change (Leach & Moore, 2019). For example, the loss in groundwater inflows would result in greater meteorological controls increasing the annual amplitude of *Tw* (O'Driscoll & DeWalle, 2006). Limiting water abstraction during low-flow periods may avoid a disconnection of groundwater/surface water exchanges and ensure environmental flows during the summer (Elmore, Null, & Mouzon, 2016). Some cooling strategies proposed to reconnect streams to floodplains and to facilitate greater lateral and hyporheic flow exchanges (Beechie et al., 2012; Daniel Caissie & Luce, 2017; Kurylyk et al., 2015) but need to be tested at a regional scale. To apply efficient and effective actions, river managers have to focus on small and medium streams and can use the environmental variables identified in our classification results as indicators to assess the climate sensitivity of unmonitored streams.

5 | CONCLUSION

In this study, we proposed a framework to compare thermal sensitivity (*TS*) for 127 stations located on temperate streams between 2008 and 2012 and to cluster stations sharing similar natural thermal regimes, not influence by anthropogenic effects. On the basis of weekly *Ta*–*Tw* relationships, four thermal regimes were identified with differing annual *Tw* in terms of magnitude and amplitudes in comparison with *Ta*. We linked each cluster to different environmental controlling factors as inferred by *TS*. This highlighted that shading from riparian vegetation, groundwater inflows, and the distance from the source of streams were the main drivers of the moderation of streams located in the Loire catchment. Streams influenced by both groundwater inflows and shading are the most moderated with the lowest *TS* and an annual amplitude of *Tw* around half the annual amplitude of *Ta*. Inversely, stations located on large streams or on streams slightly or not influenced by groundwater inflows and/or shading showed the highest *TS* and are very climate sensitive. Their *Tw* amplitude and magnitude were very close to those of *Ta*; consequently, these rivers are deemed the most sensitive to the effects of future climate change.

The *Tw* metrics and the environmental variables remain simple to determine and can easily be applied in others catchments at a regional scale. One of the perspectives to this work would be to explore if main controlling factors of the *Tw* variability identified here are the same in different climate and physiographical regions elsewhere. We observe that almost invariability streams studied in reviewed publications for linear regression models of weekly *Ta–Tw* relationship (Table 3) correspond to temperate and continental climatic regions. It would be interesting to study streams from different climatic contexts to understand how controls of *TS* may vary. Furthermore, it would be insightful to explore how *TS* may be modified by anthropogenic effects (dams, weirs, and other flow augmentation/abstractions, etc.). Management agencies can use our findings on thermal sensitivity for prioritizing restoration areas to moderate stream temperature and undertake mitigation and adaptation actions to protect sensitive aquatic species in the context of a changing environment.

DATA AVAILABILITY STATEMENT

Temperature used in this study are available from the French Biodiversity Agency (AFB; www.afbiodiversite.fr). Restrictions apply to the availability of these data, which were used under license herein. Data are available at http://www.naiades.eaufrance.fr with the permission of the French Biodiversity Agency (www.naiades.eaufrance.fr/formulaire/contact). Discharge data are available from the French river flow monitoring network (HYDRO database, http://www.hydro.eaufrance.fr/). Restrictions apply to the availability of meteorological data, which were used under license herein with the permission of Météo France (www.meteofrance.fr).

ACKNOWLEDGMENTS

The authors wish to thank the two reviewers for their valuable comments, suggestions, and positive feedback on the manuscript. The research project was funded by the French Agency for Biodiversity (AFB). Thanks are due to the AFB, the DREAL Auvergne, the DREAL Pays de Loire and the DREAL Centre for the temperature data.

ORCID

Aurélien Beaufort https://orcid.org/0000-0002-6523-8269
Florentina Moatar https://orcid.org/0000-0002-9251-6420
Eric Sauquet https://orcid.org/0000-0001-9539-7730
DavidM. Hannah https://orcid.org/0000-0003-1714-1240

REFERENCES

Arismendi, I., Johnson, S. L., Dunham, J. B., & Haggerty, R. (2013). Descriptors of natural thermal regimes in streams and their responsiveness to change in the Pacific Northwest of North America. *Freshwater Biology*, *58*(5), 880–894. https://doi.org/10.1111/fwb.12094

Arora, R., Toffolon, M., Tockner, K., & Venohr, M. (2018). Thermal discontinuities along a lowland river: The importance of urban areas and lakes. *Journal of Hydrology*, *564*, 811–823. https://doi.org/10.1016/j.jhydrol.2018.05.066

Baratelli, F., Flipo, N., & Moatar, F. (2016). Estimation of stream–aquifer exchanges at regional scale using a distributed model: Sensitivity to in-stream water level fluctuations, riverbed elevation and roughness. *Journal of Hydrology*, *542*, 686–703. https://doi.org/10.1016/j.jhydrol.2016.09.041

Beaufort, A., Lamouroux, N., Pella, H., Datry, T., & Sauquet, E. (2018). Extrapolating regional probability of drying of headwater streams using discrete observations and gauging networks. *Hydrology and Earth System Sciences*, *22*(5), 3033–3051. https://doi.org/10.5194/hess-22-3033-2018

Beaufort, A., Moatar, F., Curie, F., Ducharne, A., Bustillo, V., & Thiéry, D. (2016). River temperature modelling by Strahler order at the regional scale in the Loire River basin, France. *River Research and Applications*, *32*(4), 597–609. https://doi.org/10.1002/rra.2888

Beechie, T., Imaki, H., Greene, J., Wade, A., Wu, H., Pess, G., … Mantua, N. (2012). Restoring salmon habitat for a changing climate: Restoring salmon habitat for a changing climate. *River Research and Applications*, 939–960. https://doi.org/10.1002/rra.2590

Boisneau, C., Moatar, F., Bodin, M., & Boisneau, P. (2008). Does global warming impact on migration patterns and recruitment of Allis shad (*Alosa alosa* L.) young of the year in the Loire River, France? *Hydrobiologia*, *602*, 179–186. https://doi.org/10.1007/s10750-008-9291-6

Breiman, L. (2001). Random forests. *Machine learning*, *45*(1), 5–32. https://doi.org/10.1023/A:1010933404324

Breiman, L., Friedman, J., Stone, C. J., & Olshen, R. A. (1984). Classification and regression trees (Wadsworth International Group).

Bustillo, V., Moatar, F., Ducharne, A., Thiéry, D., & Poirel, A. (2014). A multimodel comparison for assessing water temperatures under changing climate conditions via the equilibrium temperature concept: Case study of the Middle Loire River, France. *Hydrological Processes*, *28*(3), 1507–1524. https://doi.org/10.1002/hyp.9683

Caissie, D. (2006). The thermal regime of rivers: A review. *Freshwater Biology*, *51*(8), 1389–1406. https://doi.org/10.1111/j.1365-2427.2006.01597.x

Caissie, D., & Luce, C. H. (2017). Quantifying streambed advection and conduction heat fluxes. *Water Resources Research*, *53*(2), 1595–1624. https://doi.org/10.1002/2016WR019813

Casado, A., Hannah, D. M., Peiry, J.-L., & Campo, A. M. (2013). Influence of dam-induced hydrological regulation on summer water temperature: Sauce Grande River, Argentina. *Ecohydrology*, *6*(4), 523–535. https://doi.org/10.1002/eco.1375

Chang, H., & Psaris, M. (2013). Local landscape predictors of maximum stream temperature and thermal sensitivity in the Columbia River Basin, USA. *Science of The Total Environment*, *461-462*, 587–600. https://doi.org/10.1016/j.scitotenv.2013.05.033

Chu, C., Jones, N. E., & Allin, L. (2009). Linking the thermal regimes of streams in the Great Lakes Basin, Ontario, to landscape and climate variables. *River Research and Applications*, *n/a-n/a.*, n/a. https://doi.org/10.1002/rra.1259

Comte, L., Buisson, L., Daufresne, M., & Grenouillet, G. (2013). Climate-induced changes in the distribution of freshwater fish: Observed and predicted trends. *Freshwater Biology*, *58*(4), 625–639. https://doi.org/10.1111/fwb.12081

De'ath, G., & Fabricius, K. E. (2000). Classification and regression trees: A powerful yet simple technique for ecological data analysis. *Ecology*, *81*(11), 3178–3192. https://doi.org/10.1890/0012-9658(2000)081[3178:CARTAP]2.0.CO;2

Ducharne, A. (2008). Importance of stream temperature to climate change impact on water quality. *Hydrol. Earth Syst. Sci.*, *14*.

Dugdale, S. J., Malcolm, I. A., Kantola, K., & Hannah, D. M. (2018). Stream temperature under contrasting riparian forest cover: Understanding thermal dynamics and heat exchange processes. *Science of The Total Environment*, *610-611*, 1375–1389. https://doi.org/10.1016/j.scitotenv.2017.08.198

Elmore, L. R., Null, S. E., & Mouzon, N. R. (2016). Effects of environmental water transfers on stream temperatures: Effects of environmental water transfers. *River Research and Applications*, *32*(7), 1415–1427. https://doi.org/10.1002/rra.2994

Erickson, T. R., & Stefan, H. G. (2000). Linear air/water temperature correlations for streams during open water periods. *Journal of Hydrologic Engineering*, *5*(3), 317–321. https://doi.org/10.1061/(ASCE)1084-0699(2000)5:3(317)

Eschbach, D., Piasny, G., Schmitt, L., Pfister, L., Grussenmeyer, P., Koehl, M., … Serradj, A. (2017). Thermal-infrared remote sensing of surface water–groundwater exchanges in a restored anastomosing channel (Upper Rhine River, France). *Hydrological Processes*, *31*(5), 1113–1124. https://doi.org/10.1002/hyp.11100

Fabris, L., Malcolm, I. A., Buddendorf, W. B., & Soulsby, C. (2018). Integrating process-based flow and temperature models to assess riparian forests and temperature amelioration in salmon streams. *Hydrological Processes*, *32*(6), 776–791. https://doi.org/10.1002/hyp.11454

Garner, G., Hannah, D. M., Sadler, J. P., & Orr, H. G. (2014). River temperature regimes of England and Wales: Spatial patterns, inter-annual variability and climatic sensitivity. *Hydrological Processes*, *28*(22), 5583–5598. https://doi.org/10.1002/hyp.9992

Garner, G., Hannah, D. M., & Watts, G. (2017). Climate change and water in the UK: Recent scientific evidence for past and future change. *Progress in Physical Geography: Earth and Environment*, *41*(2), 154–170. https://doi.org/10.1177/0309133316679082

Garner, G., Malcolm, I. A., Sadler, J. P., & Hannah, D. M. (2017). The role of riparian vegetation density, channel orientation and water velocity in determining river temperature dynamics. *Journal of Hydrology*, *553*, 471–485. https://doi.org/10.1016/j.jhydrol.2017.03.024

Gustard, A., Bullock, A., & Dixon, J. M. (1992). *Low flow estimation in the United Kingdom*. Wallingford: Institute of Hydrology.

Hannah, D. M., & Garner, G. (2015). River water temperature in the United Kingdom: Changes over the 20th century and possible changes over the 21st century. *Progress in Physical Geography*, *39*(1), 68–92. https://doi.org/10.1177/0309133314550669

Hannah, D. M., Malcolm, I. A., Soulsby, C., & Youngson, A. F. (2004). Heat exchanges and temperatures within a salmon spawning stream in the Cairngorms, Scotland: Seasonal and sub-seasonal dynamics. *River Research and Applications*, *20*(6), 635–652. https://doi.org/10.1002/rra.771

Hannah, D. M., Malcolm, I. A., Soulsby, C., & Youngson, A. F. (2008). A comparison of forest and moorland stream microclimate, heat exchanges and thermal dynamics. *Hydrological Processes*, *22*(7), 919–940. https://doi.org/10.1002/hyp.7003

Hennig, C. (2007). Cluster-wise assessment of cluster stability. *Computational Statistics & Data Analysis*, *52*(1), 258–271. https://doi.org/10.1016/j.csda.2006.11.025

Hennig, C. (2019). fpc: Flexible procedures for clustering. *R package version*, *2*, 2–3. Available at:. https://CRAN.R-project.org/package=fpc

Hrachowitz, M., Soulsby, C., Imholt, C., Malcolm, I. A., & Tetzlaff, D. (2010). Thermal regimes in a large upland salmon river: A simple model to identify the influence of landscape controls and climate change on maximum temperatures. *Hydrological Processes*, *24*(23), 3374–3391. https://doi.org/10.1002/hyp.7756

Imholt, C., Soulsby, C., Malcolm, I. A., Hrachowitz, M., Gibbins, C. N., Langan, S., & Tetzlaff, D. (2013). Influence of scale on thermal characteristics in a large montane river basin: Thermal dynamics at different scales. *River Research and Applications*, *29*(4), 403–419. https://doi.org/10.1002/rra.1608

Institute of Hydrology (1980). *Low flow studies. Institute of Hydrology Research Report 1*. Wallingford, UK: Institute of Hydrology.

Isaak, D. J., & Hubert, W. A. (2001). A hypothesis about factors that affect maximum summer stream temperatures across montane landscapes. *Journal of the American Water Resources Association*, *37*(2), 351–366. https://doi.org/10.1111/j.1752-1688.2001.tb00974.x

Isaak, D. J., Luce, C. H., Rieman, B. E., Nagel, D. E., Peterson, E. E., Horan, D. L., … Chandler, G. L. (2010). Effects of climate change and wildfire on stream temperatures and salmonid thermal habitat in a mountain river network. *Ecological Applications*, *20*(5), 1350–1371.

Isaak, D. J., Wenger, S. J., Peterson, E. E., Ver Hoef, J. M., Nagel, D. E., Luce, C. H., … Parkes-Payne, S. (2017). The NorWeST summer stream temperature model and scenarios for the western U.S.: A crowd-sourced database and new geospatial tools foster a user community and predict broad climate warming of rivers and streams. *Water Resources Research*, *53*(11), 9181–9205. https://doi.org/10.1002/2017WR020969

Jackson, F. L., Hannah, D. M., Fryer, R. J., Millar, C. P., & Malcolm, I. A. (2017). Development of spatial regression models for predicting summer river temperatures from landscape characteristics: Implications for land and fisheries management. *Hydrological Processes*, *31*(6), 1225–1238. https://doi.org/10.1002/hyp.11087

Jackson, F. L., Malcolm, I. A., & Hannah, D. M. (2015). A novel approach for designing large-scale river temperature monitoring networks. *Hydrology Research*, nh2015106. https://doi.org/10.2166/nh.2015.106

Jackson, F. L., Fryer, R. J., Hannah, D. M., & Malcolm, I. A. (2017). Can spatial statistical river temperature models be transferred between catchments? *Hydrology and Earth System Sciences*, *21*(9), 4727–4745. https://doi.org/10.5194/hess-21-4727-2017

Jackson, F. L., Fryer, R. J., Hannah, D. M., Millar, C. P., & Malcolm, I. A. (2018). A spatio-temporal statistical model of maximum daily river temperatures to inform the management of Scotland's Atlantic salmon rivers under climate change. *Science of The Total Environment*, *612*, 1543–1558. https://doi.org/10.1016/j.scitotenv.2017.09.010

Johnson, M. F., & Wilby, R. L. (2015). Seeing the landscape for the trees: Metrics to guide riparian shade management in river catchments. *Water Resources Research*, *51*(5), 3754–3769. https://doi.org/10.1002/2014WR016802

Jones, N. E., & Schmidt, B. J. (2018). Thermal regime metrics and quantifying their uncertainty for North American streams. *River Research and Applications*, *34*(4), 382–393. https://doi.org/10.1002/rra.3257

Jonsson, B., & Jonsson, N. (2009). A review of the likely effects of climate change on anadromous Atlantic salmon *Salmo salar* and brown trout *Salmo trutta*, with particular reference to water temperature and flow. *Journal of Fish Biology*, *75*(10), 2381–2447. https://doi.org/10.1111/j.1095-8649.2009.02380.x

Kelleher, C., Wagener, T., Gooseff, M., McGlynn, B., McGuire, K., & Marshall, L. (2012). Investigating controls on the thermal sensitivity of Pennsylvania streams. *Hydrological Processes*, *26*(5), 771–785. https://doi.org/10.1002/hyp.8186

Krider, L. A., Magner, J. A., Perry, J., Vondracek, B., & Ferrington, L. C. (2013). Air–water temperature relationships in the trout streams of southeastern Minnesota's carbonate–sandstone landscape. *JAWRA Journal of the American Water Resources Association*, *49*(4), 896–907. https://doi.org/10.1111/jawr.12046

Kurylyk, B. L., MacQuarrie, K. T. B., Linnansaari, T., Cunjak, R. A., & Curry, R. A. (2015). Preserving, augmenting, and creating cold-water thermal refugia in rivers: Concepts derived from research on the Miramichi River, New Brunswick (Canada). *Ecohydrology*, *8*(6), 1095–1108. https://doi.org/10.1002/eco.1566

Laizé, C. L. R., Bruna Meredith, C., Dunbar, M. J., & Hannah, D. M. (2017). Climate and basin drivers of seasonal river water temperature dynamics. *Hydrology and Earth System Sciences*, *21*(6), 3231–3247. https://doi.org/10.5194/hess-21-3231-2017

Lalot, E., Curie, F., Wawrzyniak, V., Baratelli, F., Schomburgk, S., Flipo, N., … Moatar, F. (2015). Quantification of the contribution of the Beauce groundwater aquifer to the discharge of the Loire River using thermal infrared satellite imaging. *Hydrology and Earth System Sciences*, *19*(11), 4479–4492. https://doi.org/10.5194/hess-19-4479-2015

Leach, J. A., & Moore, R. D. (2019). Empirical stream thermal sensitivities may underestimate stream temperature response to climate warming. *Water Resources Research*, 2018WR024236. https://doi.org/10.1029/2018WR024236

Li, G., Jackson, C. R., & Kraseski, K. A. (2012). Modeled riparian stream shading: Agreement with field measurements and sensitivity to riparian conditions. *Journal of Hydrology*, *428-429*, 142–151. https://doi.org/10.1016/j.jhydrol.2012.01.032

Liaw, A., & Wiener, M. (2002). Classification and Regression by randomForest. *2*, 5.

Loheide, S. P., & Gorelick, S. M. (2006). Quantifying stream—aquifer interactions through the analysis of remotely sensed thermographic profiles and in situ temperature histories. *Environmental Science & Technology*, *40*(10), 3336–3341. https://doi.org/10.1021/es0522074

Loicq, P., Moatar, F., Jullian, Y., Dugdale, S. J., & Hannah, D. M. (2018). Improving representation of riparian vegetation shading in a regional stream temperature model using LiDAR data. *Science of The Total Environment*, *624*, 480–490. https://doi.org/10.1016/j.scitotenv.2017.12.129

Maheu, A., Poff, N. L., & St-Hilaire, A. (2016). A classification of stream water temperature regimes in the conterminous USA: Classification of stream temperature regimes. *River Research and Applications*, *32*(5), 896–906. https://doi.org/10.1002/rra.2906

Mayer, T. D. (2012). Controls of summer stream temperature in the Pacific Northwest. *Journal of Hydrology*, *475*, 323–335. https://doi.org/10.1016/j.jhydrol.2012.10.012

Moatar, F., Ducharne, A., Thiéry, D., Bustillo, V., Sauquet, E., & Vidal, J. P. (2010). La Loire à l'épreuve du changement climatique. *Géosciences*, *12*, 78–87. http://www.brgm.fr/dcenewsFile?ID=1306

Moatar, F., & Gailhard, J. (2006). Water temperature behaviour in the River Loire since 1976 and 1881. *Comptes Rendus Geoscience*, *338*(5), 319–328. https://doi.org/10.1016/j.crte.2006.02.011

Mohseni, O., & Stefan, H. G. (1999). Stream temperature/air temperature relationship: A physical interpretation. *Journal of hydrology*, *218*(3), 128–141.

Mohseni, O., Stefan, H. G., & Erickson, T. R. (1998). A nonlinear regression model for weekly stream temperatures. *Water Resources Research*, *34*(10), 2685–2692. https://doi.org/10.1029/98WR01877

Morrill, J. C., Bales, R. C., & Conklin, M. H. (2005). Estimating stream temperature from air temperature: Implications for future water quality. *Journal of Environmental Engineering*, *131*(1), 139–146. https://doi.org/10.1061/(ASCE)0733-9372(2005)131:1(139)

Nelitz, M. A., MacIsaac, E. A., & Peterman, R. M. (2007). A science-based approach for identifying temperature-sensitive streams for rainbow trout. *North American Journal of Fisheries Management*, *27*(2), 405–424. https://doi.org/10.1577/M05-146.1

O'Driscoll, M. A., & DeWalle, D. R. (2004). Stream–air temperature relationships as indicators of groundwater inputs. *2*(6), 5.

O'Driscoll, M. A., & DeWalle, D. R. (2006). Stream–air temperature relations to classify stream–ground water interactions in a karst setting, central Pennsylvania, USA. *Journal of Hydrology*, *329*(1-2), 140–153. https://doi.org/10.1016/j.jhydrol.2006.02.010

Pilgrim, J. M., Fang, X., & Stefan, H. G. (1998). Stream temperature correlations with air temperatures in Minnesota: Implications for climate warming. *Journal of the American Water Resources Association*, *34*(5), 1109–1121. https://doi.org/10.1111/j.1752-1688.1998.tb04158.x

Quintana-Seguí, P., Le Moigne, P., Durand, Y., Martin, E., Habets, F., Baillon, M., … Morel, S. (2008). Analysis of near-surface atmospheric variables: Validation of the SAFRAN analysis over France. *Journal of Applied Meteorology and Climatology*, *47*(1), 92–107. https://doi.org/10.1175/2007JAMC1636.1

Ripley, B. D. (1996). *Pattern recognition and neural networks*. Cambridge; New York: Cambridge University Press.

Rivers-Moore, N. A., Dallas, H. F., & Morris, C. (2013). Towards setting environmental water temperature guidelines: A South African example. *Journal of Environmental Management*, *128*, 380–392. https://doi.org/10.1016/j.jenvman.2013.04.059

Sinokrot, B. A., & Stefan, H. G. (1993). Stream temperature dynamics: Measurements and modeling. *Water Resources Research*, *29*(7), 2299–2312. https://doi.org/10.1029/93WR00540

Stefan, H. G., & Preud'homme, E. B. (1993). Stream temperature estimation from air temperature. *Journal of the American Water Resources Association*, *29*(1), 27–45. https://doi.org/10.1111/j.1752-1688.1993.tb01502.x

Tague, C., Farrell, M., Grant, G., Lewis, S., & Rey, S. (2007). Hydrogeologic controls on summer stream temperatures in the McKenzie River basin, Oregon. *Hydrological Processes*, *21*(24), 3288–3300. https://doi.org/10.1002/hyp.6538

Therneau, T., & Atkinson, B. (2018). rpart: Recursive partitioning and regression trees. R package version. *4*, 1–13. https://CRAN.R-project.org/package=rpart

Torgersen, C. E., Ebersole, J. L., & Keenan, D. M. (2012). Primer for identifying cold-water refuges to protect and restore thermal diversity in riverine landscapes. U.S. Environmental Protection Agency, EPA 910-C-12-001, 91.

Valette, L., Piffady, J., Chandesris, A., & Souchon, Y. (2012). SYRAH-CE: description des données et modélisation du risque d'altération de l'hydromorphologie des cours d'eau pour l'Etat des lieux DCE. Rapport final, Pôle Hydroécologie des cours d'eau Onema-Irstea Lyon. MALY-LHQ, Lyon.

van Vliet, M. T. H., Franssen, W. H. P., Yearsley, J. R., Ludwig, F., Haddeland, I., Lettenmaier, D. P., & Kabat, P. (2013). Global river discharge and water temperature under climate change. *Global Environmental Change*, *23*(2), 450–464. https://doi.org/10.1016/j.gloenvcha.2012.11.002

Vidal, J.-P., Martin, E., Franchistéguy, L., Baillon, M., & Soubeyroux, J.-M. (2010). A 50-year high-resolution atmospheric reanalysis over France with the Safran system. *International Journal of Climatology*, *30*(11), 1627–1644. https://doi.org/10.1002/joc.2003

Watts, G., Battarbee, R. W., Bloomfield, J. P., Crossman, J., Daccache, A., Durance, I., … Wilby, R. L. (2015). Climate change and water in the UK—Past changes and future prospects. *Progress in Physical Geography: Earth and Environment*, *39*(1), 6-28. https://doi.org/10.1177/0309133314542957

Wawrzyniak, V., Piégay, H., & Poirel, A. (2012). Longitudinal and temporal thermal patterns of the French Rhône River using Landsat ETM+ thermal infrared images. *Aquatic Sciences*, *74*(3), 405–414. https://doi.org/10.1007/s00027-011-0235-2

Webb, B. W., Hannah, D. M., Moore, R. D., Brown, L. E., & Nobilis, F. (2008). Recent advances in stream and river temperature research. *Hydrological Processes*, *22*(7), 902–918. https://doi.org/10.1002/hyp.6994

Wehrly, K. E., Wiley, M. J., & Seelbach, P. W. (1998). Landscape-based models that predict July thermal characteristics of lower Michigan rivers. *Michigan Department of Natural Resources*, *2037*, 24.

How to cite this article: Beaufort A, Moatar F, Sauquet E, Loicq P, Hannah D. Influence of landscape and hydrological factors on stream–air temperature relationships at regional scale. *Hydrological Processes*. 2019;1–15. https://doi.org/10.1002/hyp.13608